Journal of Molecular Catalysis A: Chemical 302 (2009) 107–111

Contents lists available at ScienceDirect

Journal of Molecular Catalysis A: Chemical

journal homepage: www.elsevier.com/locate/molcata

Adsorption and photocatalytic degradation of bilirubin on hydroxyapatite coatings with nanostructural surface

Zhengpeng Yang*, Chunjing Zhang

Institute of Materials Science and Engineering, Henan Polytechnic University, Jiaozuo 454000, China

ARTICLE INFO

Article history:
Received 8 October 2008
Received in revised form 1 December 2008
Accepted 1 December 2008
Available online 6 December 2008

Keywords:
Bilirubin
Nanostructural hydroxyapatite coatings
Adsorption
Photocatalytic degradation
Quartz crystal microbalance

ABSTRACT

Bilirubin produced from hemoglobin metabolism and normally conjugated with albumin is a kind of lipophilic endotoxin, and can cause various diseases when its concentration is high. Bilirubin adsorption on nanostructural hydroxyapatite coatings was investigated using quartz crystal microbalance (QCM) technique, and factors affecting its adsorption such as bilirubin concentration and thickness of hydroxyapatite coatings were discussed in detail. The adsorption kinetic parameter estimated from the in situ frequency measurement is about $3.59 \times 10^7\ M^{-1}$. With the present method, the photocatalytic degradation of adsorbed bilirubin under UV irradiation was investigated and discussed as well, and a photocatalytic mechanism has been proposed. The obtained information suggests that QCM is a useful method for monitoring the adsorption/degradation behavior of bilirubin on nanostructural hydroxyapatite coatings, and that nanostructural hydroxyapatite coatings which is used as adsorbent for the removal of bilirubin can be photochemically regenerated due to the degradation of adsorbed bilirubin.

© 2008 Elsevier B.V. All rights reserved.

1. Introduction

Bilirubin is one of the common metabolites of hemoglobin and is released into blood due to the destruction of red blood cells [1,2]. Normally, it is conjugated with albumin to form a water-soluble complex and excreted from hepatocytes into bile mainly as bilirubin glucuronides [3–5]. However, it has been suggested that it is toxic when the amount of bilirubin in body exceeds the binding capacity of albumin, extra free bilirubin binds and deposits to various tissues, especially in the brain. Its deposition and accumulation in tissues will cause disorders in the metabolism of bilirubin and lead to jaundice or kernicterus [6,7]. This may cause cell death in various tissues, mental retardation, celebral palsy or death [8,9]. In order to prevent these conditions, several techniques have been used for the removal of bilirubin directly from plasma of patients suffering from hyperbilirubinemia, such as haemoperfusion, haemodialysis and affinity membrane chromatography [10–13]. Of these, Haemoperfusion treatment, i.e., circulation of blood through an extracorporeal unit containing an adsorbent system for bilirubin is the most promising technique at present. Naturally, the adsorbents should have high adsorption capacity, good biocompatibility and blood compatibility, adequate mechanical and physical stability. Activated charcoal, agar, ion-exchange resin and titania have been used as adsorbents in haemoperfusion columns [14–18]. In recent years, hydroxyapatite, a main constituent of bones and teeth, has been used extensively in such fields as bone repairs, bone implant, bioactive materials and purification and separation of biological molecules and organic contaminants due to its excellent biocompatibility, slow biodegradation, good mechanical stability, great sorption property and heterogeneous photocatalytic degradation under UV irradiation [19–23]. Similarly, it can be expected that the nanostructural hydroxyapatite coatings can be used to adsorb and photocatalytically decompose bilirubin when it is used as adsorbents in the haemoperfusion columns. To the best of our knowledge, it has not still been reported in literatures about the adsorption and degradation of bilirubin on nanostructural hydroxyapatite coatings.

In the present work, to obtain a direct and comprehensive understanding of the adsorption and degradation of bilirubin on nanostructural hydroxyapatite coatings, quartz crystal microbalance (QCM) technology, which is capable of measuring the nanogram level of mass change on the surface and has been successfully used for the study of adsorption/desorption process at solid/solution interface [24–26], has been employed to in situ monitor the interaction between bilirubin and hydroxyapatite. The information obtained is essential for application of nanostructural hydroxyapatite to blood purification therapy.

2. Experimental

2.1. Materials

Bilirubin IX-α (93%) was purchased from Sigma Chemical Co., and used without further purification. Nanostructural

* Corresponding author. Tel.: +86 391 3983000.
E-mail address: zhengpengyang@yahoo.com.cn (Z. Yang).

1381-1169/$ – see front matter © 2008 Elsevier B.V. All rights reserved.
doi:10.1016/j.molcata.2008.12.001

hydroxyapatite powder was prepared according to the method described elsewhere [27]. All other chemicals were of analytical grade purchased from Shanghai Chemical Co., China. Deionized (DI) water (resistivity of 18 MΩ cm) was obtained from a Milli-Q system (Millipore Inc.), and was used for rinsing and for makeup of all aqueous solutions.

Bilirubin stock solution (1 mM) was prepared daily by dissolving 5.8 mg of bilirubin in 10 ml of 50 mM NaOH solution. Standard solutions of lower concentrations were prepared by further dilution of the bilirubin stock solution. All solutions were stored in amber glass vials wrapped with aluminum foil and placed in the dark to prevent light-initiated bilirubin oxidation. The pH of the solutions was adjusted by adding an adequate amount of dilute HCl. Bilirubin solution (pH 7.4, 37 °C) was used in our experiments, unless otherwise stated.

2.2. Apparatus

QCM measurements were performed using a Q-sense instrument (Gothenburg, Sweden). Mechanically polished AT-cut 9-MHz quartz crystals (diameter of 12 mm, Beijing Chenjing Co., Beijing, China) were vacuum deposited with gold electrodes (6-mm diameter) on both sides of the surface. To reduce background frequency drift, one electrode was completely insulated from the test liquid. This was accomplished by mounting a glass cover slip over one side of the quartz crystal, which was held in place by two silicon o-rings. The o-rings were large enough (10 mm) so that they could make contact only with the exposed quartz peripheral to the centrally located electrode and not with the electrode itself. Thus, the covered electrode was in contact only with air. This covering assembly was held in place using silicone glue. The electrical contacts were insulated from the test solution using silicon tubing and silicon glue, and only one electrode was exposed to the test solution. The working crystal was connected to an IC-TTL oscillator. Both the detector cell and the oscillator were put in a copper Faradaic cabin to remove the surrounding electromagnetic noise. The frequency was monitored by a frequency counter (Iwatsu, Model SC-7201), and the recorded data were stored in a computer.

IR spectrum was recorded using Fourier transformed infrared spectroscopy (FTIR: Model 883, PerkinElmer Optoelectronics Inc., USA).

2.3. Preparation of nanostructural hydroxyapatite coatings at the surface of quartz crystal

Aqueous suspensions of nanostructural hydroxyapatite particles were prepared as given in detail elsewhere [28]. Nanostructural hydroxyapatite powder was firstly dispersed into DI water, and then oscillated by ultrasonic irradiation for 1 h to form hydroxyapatite suspension. After the gold-plated quartz crystals were treated with 3 M NaOH solution for 20 min and washed with water, the nanostructural hydroxyapatite coatings at the surface of quartz crystal were prepared using the hydroxyapatite suspension by spin coating at 3500 rpm for 3 min. Thicker coatings were achieved by repeating the coating process. A narrow strip of the nanostructural hydroxyapatite coatings at the edge of the quartz crystal was removed using a methanol-soaked tissue. Before and after the nanostructural hydroxyapatite coating modification, the frequency of the quartz crystal was measured, and the thickness of nanostructural hydroxyapatite coatings was estimated from the amount of deposited hydroxyapatite particles. The nanostructural hydroxyapatite coatings with 1.0 μm thickness were employed in our study, unless otherwise stated. The coatings were finally heat-treated at 400 °C for 3 h in order to consolidate the coupling of hydroxyapatite and gold surface.

2.4. Adsorption of bilirubin at the surface of nanostructural hydroxyapatite coatings

To monitor the in situ adsorption process of bilirubin at the surface of nanostructural hydroxyapatite coatings, the following procedure was adopted. After mounting the crystal in the cell, a small amount of DI water was introduced into the cell. When the frequency became stable, the bilirubin aqueous solution was introduced into the cell within 5 s. Time-dependent change in the frequency was recorded continuously by a frequency counter and stored in a microcomputer during the adsorption process of bilirubin.

2.5. Photocatalytic degradation of bilirubin adsorbed onto nanostructural hydroxyapatite coatings

The photocatalytic experiments of bilirubin adsorbed onto nanostructural hydroxyapatite coatings were carried out by UV illumination. The change in frequency with time was recorded by QCM equipment.

3. Results and discussion

3.1. Adsorption of bilirubin on nanostructural hydroxyapatite coatings

FTIR spectroscopy proved to be useful to characterize bilirubin adsorption on nanostructural hydroxyapatite coatings. Fig. 1 shows the FTIR spectra of hydroxyapatite after soaking in 1.0 μM bilirubin solution (pH 7.4) for 2 h at 37 °C. It was found after soaking that all characteristic bands of bilirubin and hydroxyapatite appeared in the IR spectrum of hydroxyapatite/bilirubin. For example, strong and medium intensity bands of bilirubin at 3400, 3261, 2913, 1696, 1647, 1612, 1249, 989 and 945 cm^{-1}. These IR bands are attributed to the NH stretching mode, asymmetric OH stretching, asymmetric CH stretching in the CH_2 group, the carboxylic C=O stretching mode, C=O stretching mode, C=C stretching vibration, C–C and C–N bonds, the methyl groups and C–H bending mode of bilirubin, respectively. In addition, three obvious bands at 1100, 1050 and 566 cm^{-1} are assigned to the stretching mode of PO_4^{3-} groups. IR analysis not only strongly confirmed the adsorption of bilirubin on nanostructural hydroxyapatite coatings, but also indicated that no obvious change occurred in HAP and bilirubin groups in

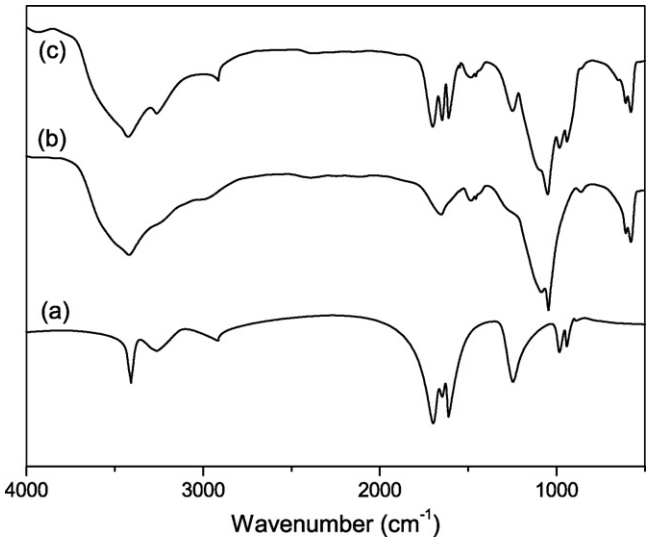

Fig. 1. Infrared spectra of (a) bilirubin, (b) hydroxyapatite and (c) hydroxyapatite/bilirubin.

Table 1
The amount of bilirubin adsorbed on nanostructural hydroxyapatite coatings.

Thickness of coatings (μm)[a]	$\Delta F_{sol.}$ (Hz)[b]	$\Delta F_{air.}$ (Hz)[c]	Mass of adsorbed bilirubin (μg)
0.4	125 ± 3.7	69 ± 1.4	0.046 ± 0.001
0.8	210 ± 9.5	106 ± 5.1	0.071 ± 0.003
1.0	241 ± 13.2	118 ± 4.5	0.079 ± 0.003
1.2	263 ± 11.2	124 ± 3.9	0.083 ± 0.002

1.0 μM bilirubin (pH 7.4); 37 °C.

[a] Estimated from the values of frequency shift corresponding to the hydroxyapatite coatings based on the mass sensitivity of ~5.7 ng Hz^{-1} cm^{-2} of 9 MHz quartz crystal and the density of hydroxyapatite at 3.16 g cm^{-3}.

[b] Measured in aqueous solution before/after the crystals were incubated in bilirubin solution for 2 h (mean ± S.D., n = 3).

[c] Measured in dry nitrogen before/after the crystals were incubated in bilirubin solution for 2 h (mean ± S.D., n = 3).

the process of bilirubin adsorption, namely bilirubin adsorption on nanostructural hydroxyapatite coatings was a physical adsorption process.

The mass of bilirubin adsorbed on various thickness of hydroxyapatite coatings was estimated, and the results were presented in Table 1. Frequency shifts corresponding to the adsorbed bilirubin on nanostructural hydroxyapatite coatings were measured in a dry nitrogen stream ($\Delta F_{air.}$) and in an aqueous solution ($\Delta F_{sol.}$), respectively. The value of $\Delta F_{sol.}$ is larger than that of $\Delta F_{air.}$ because $\Delta F_{sol.}$ includes additional frequency shifts due to water and ions incorporated in the adsorbed layer and the associated changes in the interfacial properties (e.g., surface morphology, hydrophobicity/hydrophilicity). According to the value of $\Delta F_{air.}$ (it is more reasonable for use in the calculation of the adsorbed bilirubin), the mass of adsorbed bilirubin can be calculated. It was found that the mass of adsorbed bilirubin increased with the increasing thickness of hydroxyapatite coatings, indicating that bilirubin can enter into the inner layer of the hydroxyapatite coatings due to the porous structure of nanostructural hydroxyapatite coatings.

Our study indicated that bilirubin concentration had a significant effect on the amount of bilirubin adsorbed onto nanostructural hydroxyapatite coatings with 1.0 μM thickness. As seen in Fig. 2, the amount of adsorbed bilirubin increased rapidly with the increase in bilirubin concentration in the range of 0.2–1.0 μM, and the maximum of adsorbed bilirubin was approximately 0.08 μg in 1.0 μM bilirubin solution. However, a slight increase in adsorption amount was observed at bilirubin concentration above 1.0 μM. The relation

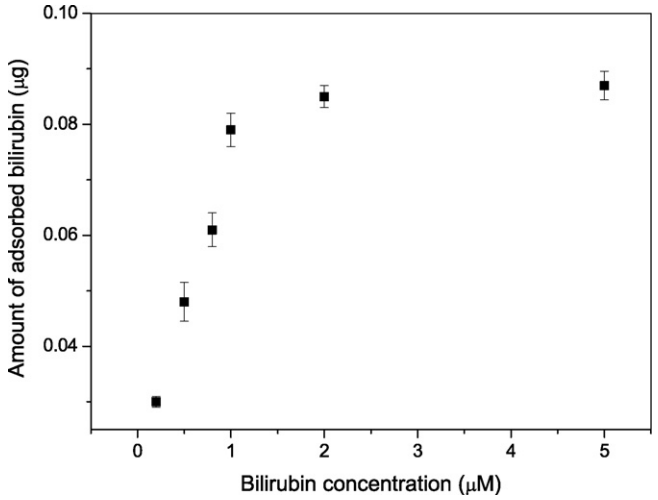

Fig. 2. Effect of bilirubin concentration on the amount of bilirubin adsorbed onto nanostructural hydroxyapatite coatings. 37 °C; pH 7.4; average of three experiments (mean ± S.D.).

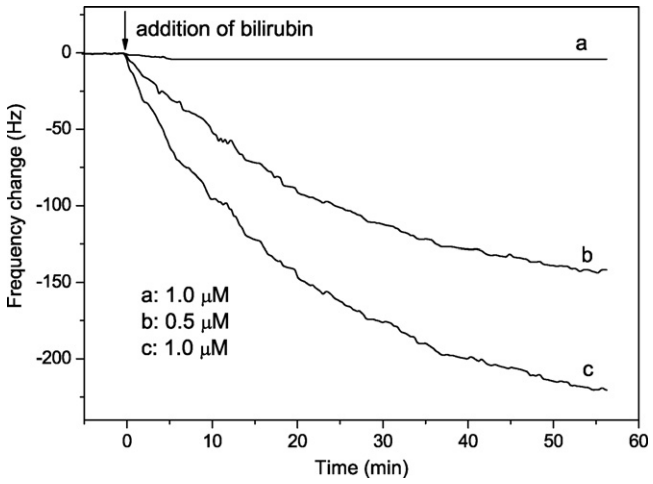

Fig. 3. Frequency change of QCM after the addition of bilirubin solution (pH 7.4, 37 °C) to the detector cell. Quartz crystal (a) with Au electrode; (b) with hydroxyapatite/Au; (c) with hydroxyapatite/Au.

between adsorption amount and bilirubin concentration suggested that saturation adsorption concentration of bilirubin on nanostructural hydroxyapatite coatings was 1.0 μM. 1.0 μM bilirubin was exployed in our study, unless otherwise stated.

3.2. Kinetics of bilirubin adsorption on nanostructural hydroxyapatite coatings

The frequency change of QCM with time was monitored at various concentrations of bilirubin at pH 7.4 (Fig. 3). In comparison with the response to the bare gold electrode, a larger frequency response to the adsorption of bilirubin was observed on nanostructural hydroxyapatite coatings and a longer time was required for the crystal to attain a frequency plateau. Considering that in situ frequency measurement includes additional frequency changes caused by over-adsorption and the change in the property of nanostructural hydroxyapatite coatings, the adsorption rate constant rather than the total frequency change was used to characterize the adsorption behavior of bilirubin on hydroxyapatite coatings. Assuming that the interaction between the remaining unbound sites on nanostructural hydroxyapatite (H) coatings and bilirubin (B) in solution follows the pseudo-first-order kinetics as shown below:

$$H + B \rightleftharpoons HB \quad (1)$$

The reaction rate can be described as

$$\frac{d[HB]}{dt} = k_a[H][B] - k_d[HB] \quad (2)$$

where k_a and k_d are the association constant and the dissociation constant, respectively. Δf ($\Delta f = f_0 - f$) is proportional to [HB], and $\Delta f_m - \Delta f$ to [H] (Δf_m = the maximum value of frequency change).Thus, Eq. (2) can be expressed as

$$\frac{d(\Delta f)}{dt} = k_a C(\Delta f_m - \Delta f) - k_d(\Delta f) \quad (3)$$

where C is the concentration of bilirubin assumed to be a constant in the test solution. For the estimation of k_a and k_d, the values of $d(\Delta f)/dt$ were plotted against the corresponding Δf (see Fig. 4, corresponding to curves of Fig. 3). The slope (SL) and intercept (INT) of the line are related to the kinetic constants, i.e., SL = $-(k_aC + k_d)$ and INT = $k_a \Delta f_m C$.

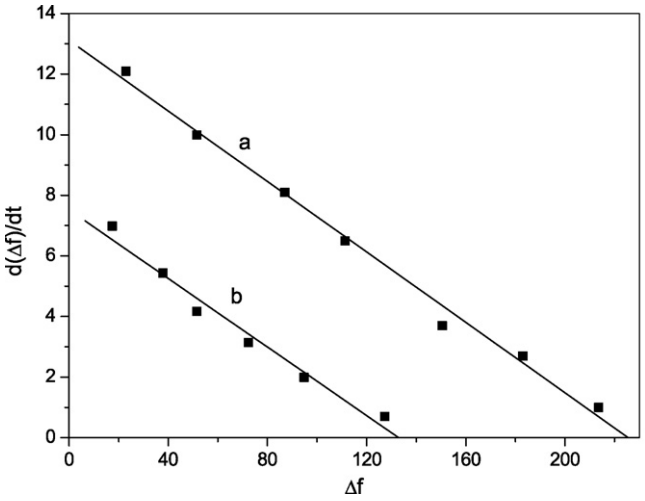

Fig. 4. Plot of d(Δf)/dt vs. Δf. (a) Corresponding to curve (c) of Fig. 3; (b) corresponding to curve (b) of Fig. 3.

The equilibrium constant K for the formation of the hydroxyapatite/bilirubin complex could be estimated as follow:

$$K = \frac{k_a}{k_d} \quad (4)$$

The value of K obtained from Fig. 4 is $3.57 \times 10^7\ M^{-1}$ in 0.5 μM bilirubin solution and the value of K is $3.72 \times 10^7\ M^{-1}$ in 1.0 μM bilirubin solution. The two values are approximately equal, indicating that the interaction between hydroxyapatite and bilirubin is independent on the change in the bilirubin concentration.

3.3. Photocatalytic degradation of bilirubin adsorbed on nanostructural hydroxyapatite coatings

Fig. 5 shows the process for the removal of adsorbed bilirubin on nanostructural hydroxyapatite coatings by UV illumination. Bilirubin solution (1.0 μM, pH 7.4) was firstly introduced into the cell and left to adsorb until reaching adsorption equilibrium (stage I), the crystal surface was then rinsed with two successive additions of DI water (stage II), finally the crystal was illuminated with UV light (stage III). Introduction of bilirubin leaded to a rapid decrease in frequency due to immediate and rapid adsorption of bilirubin

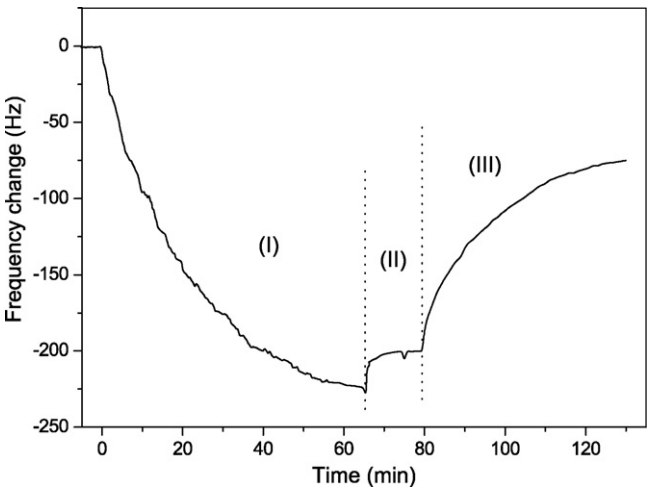

Fig. 5. Plot of frequency change against time. (I) bilirubin adsorption, (II) rinsing with DI water, (III) degradation of bilirubin during UV illumination. 1.0 μM bilirubin (pH 7.4); 37 °C.

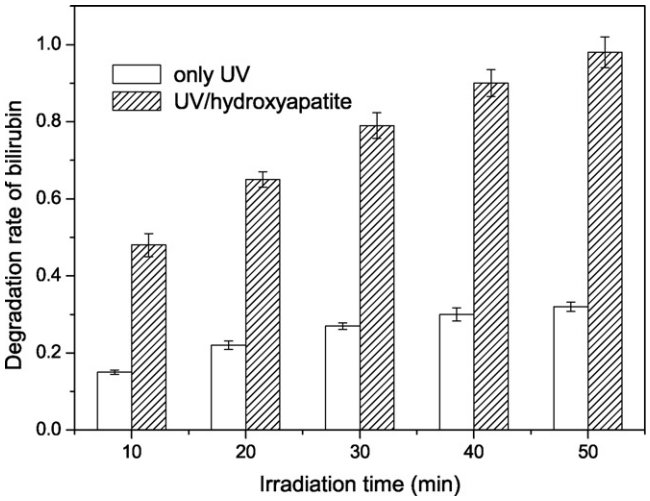

Fig. 6. Effect of UV and hydroxyapatite on the photocatalytic degradation of bilirubin. 20 μM bilirubin (pH 7.4); 0.1 g/L hydroxyapatite; 37 °C; average of three experiments (mean ± S.D.).

on nanostructural hydroxyapatite coatings. A small increase in frequency was observed during rinsing, this could be attributed to that the rinsing process may remove weakly bound bilirubin which was loosely associated with nanostructural hydroxyapatite coatings. UV illumination resulted in an immediate increase in frequency, indicating a rapid removal of adsorbed bilirubin from nanostructural hydroxyapatite coatings. To further understand the role of nanostructural hydroxyapatite in the process of bilirubin removal, the degradation of bilirubin in the presence and absence of hydroxyapatite during UV irradiation was investigated. The degradation rate was estimated according to the change in bilirubin concentration in solution before and after degradation. Our study indicated that degradation of bilirubin was related to hydroxyapatite. As

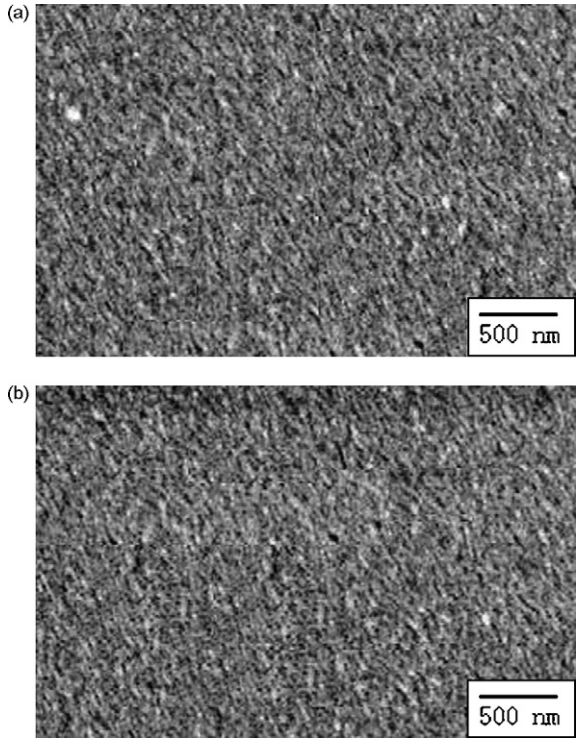

Fig. 7. SEM micrographs of nanostructural hydroxyapatite coatings before bilirubin adsorption (a) and after degradation of adsorbed bilirubin (b).

seen in Fig. 6, the degradation rate was higher in the presence of hydroxyapatite and it was found that bilirubin in solution was almost degraded completely at 50 min irradiation time. This was in high contrast with the 32.0% degradation obtained under the same experiment performed in the absence of hydroxyapatite. The results demonstrated that hydroxyapatite could accelerate bilirubin degradation during UV illumination. The degradation process can be explained as follows. When hydroxyapatite is illuminated with UV light, the photo-induced electronic excitation will happen, the electronic state of the surface PO_4^{3-} group will change and create a vacancy on hydroxyapatite and the electron is transferred to the surrounding oxygen followed by the formation of $^{\bullet}O_2^{-}$ radicals. The generated superoxide radical is a powerful oxidizing agent, which can not only oxidize the bilirubin molecules, but react with water molecules and $^{-}$OH ions and produce $^{\bullet}$OH radicals which will further oxidize the bilirubin molecules present at or near the surface of hydroxyapatite. The obtained results indicates that nanostructural hydroxyapatite coatings not only can adsorb bilirubin, but able to degrade thoroughly the adsorbed bilirubin. Fig. 7 shows the surface morphology of hydroxyapatite coatings before bilirubin adsorption and after degradation of adsorbed bilirubin, no obvious change was observed after the photodegradation of bilirubin. Such results further confirm that nanostructural hydroxyapatite coatings can be completely regenerated, and reused for the adsorption and degradation of bilirubin.

4. Conclusions

The adsorption of bilirubin onto nanostructural hydroxyapatite coatings has been verified by IR spectra. QCM measurements indicate the amount of adsorbed bilirubin increases with the increase in bilirubin concentration and thickness of hydroxyapatite coatings. The adsorption kinetic parameter (K) estimated from the frequency measurements is approximately $3.59 \times 10^7\ M^{-1}$, and the value of K is independent on the change in bilirubin concentration. During UV illumination, the frequency changes of QCM indicate that adsorbed bilirubin can be photochemically degraded due to the generation of radicals at the surface of nanostructural hydroxyapatite. The obtained results are of great importance for application of nanostructural hydroxyapatite to blood purification therapy.

References

[1] Z.P. Yang, S.H. Si, C.J. Zhang, G. Song, J. Colloid Interf. Sci. 305 (2007) 1.
[2] T. Asano, K. Tsuru, S. Hayakawa, A. Osaka, Acta Biomater. 4 (2008) 1067.
[3] Y. Andreu, M. Ostra, C. Ubide, J. Galban, S. de Marcos, J.R. Castillo, Talanta 57 (2002) 343.
[4] X. Wang, J.R. Chowdhury, N.R. Chowdhury, Curr. Paediatr. 16 (2006) 70.
[5] Z.P. Yang, S.H. Si, Y.S. Fung, Thin Solid Films 515 (2007) 3344.
[6] B. Zietz, T. Gillbro, J. Phys. Chem. B 111 (2007) 11997.
[7] M.A. Brito, R.F.M. Silva, D. Brites, Clin. Chim. Acta 374 (2006) 46.
[8] A. Lavin, C. Sung, A.M. Klibanov, R. Langer, Science 230 (1985) 543.
[9] A.S. Falcäo, R.F.M. Silva, A. Fernandes, M.A. Brito, D. Brites, Brain Res. 1149 (2007) 191.
[10] L. Zhang, G. Jin, J. Chromatogr. B 821 (2005) 112.
[11] S. Senel, F. Denizli, H. Yavuz, A. Denizli, Sep. Sci. Technol. 37 (2002) 1989.
[12] K. Filip, J. Maly, J. Horky, M. Tiustakova, J. Kalal, M. Vrana, Czech Med. 13 (1990) 34.
[13] K. Morishita, H. Yokoyama, S. Inoue, T. Koshino, Y. Tamiya, T. Abe, Eur. J. Cardiothor. Surg. 15 (1999) 502.
[14] Y.M. Cai, X.J. Tang, C.X. Xia, Z.M. Li, J. Microencapsul. 8 (1991) 327.
[15] M.C. Annesini, C.D. Carlo, V. Piemonte, L. Turchetti, Biochem. Eng. J. 40 (2008) 205.
[16] S. Sideman, L. Mor, D. Mordohovich, M. Mihich, O. Zinder, M.J. Brandes, J. Trans. Am. Soc. Artif. Int. Organs 27 (1981) 434.
[17] S. Faenza, M. Balestri, G. Martinelli, M. Spighi, M. Fini, R. Giardino, Int. J. Artif. Organs 15 (1992) 677.
[18] T. Asano, S. Takemoto, K. Tsuru, S. Hayakawa, A. Osaka, S. Takashima, J. Ceram. Soc. Jpn. 111 (2003) 645.
[19] C.X. Wang, M. Wang, X. Zhou, Biomaterials 24 (2003) 3069.
[20] Z.P. Yang, S.H. Si, X.M. Zeng, C.J. Zhang, H.J. Dai, Acta Biomater. 4 (2008) 560.
[21] J.W. Shen, T. Wu, Q. Wang, H.H. Pan, Biomaterials 29 (2008) 513.
[22] K. Kandori, S. Tsuyama, H. Tanaka, T. Ishikawa, Colloid Surf. B 58 (2007) 98.
[23] M.P. Reddy, A. Venugopal, M. Subrahmanyam, Appl. Catal. B: Environ. 69 (2007) 164.
[24] K.S. Kontturi, T. Tammelin, L.S. Johansson, P. Stenius, Langmuir 24 (2008) 4743.
[25] W.R. Glomm, O. Halskau, A.M.D. Hanneseth, S. Volden, J. Phys. Chem. B 111 (2007) 14329.
[26] S.H. Si, L. Si, F.L. Ren, D.R. Zhu, Y.S. Fung, J. Colloid Interf. Sci. 253 (2002) 47.
[27] P. Parhi, A. Ramanan, A.R. Ray, Mater. Lett. 58 (2004) 3610.
[28] Q. Yang, Y.Y. Zhang, M.L. Liu, M. Ye, Y.Q. Zhang, S.Z. Yao, Anal. Chim. Acta 597 (2007) 58.